EUROPEAN WORKING GROUP "HOT LABORATORIES AND REMOTE HANDLING"
September 27-29, 2000
PSI, Villigen, Switzerland

A micro beam collimator for high-resolution XRD investigations

D.PAPAIOANNOU, J. SPINO
Institute for Transuranium Elements
P.O.Box 2340, D-76125 Karlsruhe
Germany

Abstract

Based on the necessity of obtaining crystallographic information from the some hundred micrometers thin periphery (rim) zone of irradiated nuclear fuel pellets, a collimating system has been developed for condensing X-rays, providing a very thin but intense and low divergent flat beam with a nominal aperture of 15 μm x 4000 μm (linear-shape cross section). Owing to the high brilliance win, the condenser can be operated even with a conventional CuKα-radiation tube, e.g. in a common Bragg-Brentano diffractometer. Acquisition of XRD patterns on very thin layers of materials (20-30 μm) can be thus carried out in the laboratory without need of high-intensity radiation sources (e.g. synchrotron), as demanded by most approaches using glass capillary collimators. The concentrator has been mounted in a powder diffractometer installed in a lead-shielded glove box used as a hot cell for examinations of toxic and radioactive samples. In the paper presented, the apparatus will be described and some novel micro-XRD observations on UO_2 spent fuels will be discussed, that yielded important information on structural changes occurring along the pellet radius at high burn-ups.

1. Introduction

Concentrators (or condensers) producing high intensity X-ray beams in the micrometer size are valuable tools in many industrial and scientific fields. Applications of micro focusing techniques are increasingly reported in metal refining, semiconductor and ceramic industry, as well as in biological and medical sciences [1,2]. Also, use of micro beams in several types of techniques, such as diffraction, spectroscopy or microscopy, improves their resolution and increases their applicability in many individual cases [1,2].

Constructively, many limitations and technical difficulties overwhelm hard X-ray micro beam formation. Contrary to visible light, X-ray focusing optics can not be based on conventional lenses, since the refractive index *n* for the air/solid interface is slightly less than unity. Also, due to this property, an X-ray striking a plane smooth surface will be reflected only if the incident angle remains lower than a critical θ_c[1] [3,4]. Detailed description of these phenomena can be found in many fundamental physics books [5,6] and so will not be mentioned further in this text.

Most approaches for parallel micro beam generation are then based on the multiple total reflection of X-rays, usually inside lead-glass capillaries [1-4,7,8]. Directing the source X-rays towards the capillary tube entrance, the incident beam may be compressed, as long as the angle of incidence for each reflection remains below the critical value θ_c. For lead glass and X-ray photons of 8 KeV, θ_c does not exceed 3 mrad (0.17°) [9]. Practically, this means that a tapered (lead glass) capillary of about 10 cm length will be limited to an entrance opening of about 20-50 μm, if an output beam size of 3-11 μm is required [1,7]. Hence, only an extremely small amount of the incident radiation can be condensed, for which micro-beam experiments of this kind require high input X-ray intensities and are usually performed with high-energy synchrotron radiation sources.

2. The present development

The aim of the present approach was to provide a technique for X-ray beam compression and focusing capable of being used in a conventional X-ray diffractometer with the Bragg-Brentano geometry, so as to enable the characterisation of very small sample regions without need of very large radiation sources (synchrotron).

---

[1] In the simplified form: $\theta_c=(2\delta)^{1/2}$ and $\delta=(N\, e^2\, \lambda^2\, Z\, \rho\, /(2\, \pi\, m\, c^2\, A)$, where N =Avogadro's number, e= electron charge, λ= wave length of radiation, Z=atomic number, ρ=material density, m=electron mass, c=velocity of light and A=atomic mass

A possibility of increasing the amount of radiation that can be condensed is to use reflecting materials with higher θ_c, such that larger portion of the incident beam is intersected by the condenser. Ideal materials for such a purpose are the heavyweight metals with high electron density[2] [2]. In addition, metals exhibit higher mechanical strength than glass, allowing more stable and larger capillary-type constructions. Thus, the efficiency of the condenser can be increased, since the longer the capillary and the larger its inlet aperture, the bigger the amount of radiation that can be captured and compressed. These concepts have been considered and successfully applied in the present invention, which deals with a capillary type construction.

An important aspect taken into account in this development is that in XRD observations of polycrystalline materials using Bragg-Brentano diffractometers, only the grains oriented parallel to the sample surface and therefore coincident with the zero position of the apparatus contribute to the diffracted intensity. Since in solid materials the grain size is in general in the micrometer range, it is only by chance that favourably oriented grains are illuminated when using cross-sectional micro-beam from capillary tubes, such that in this case, not only the incident but also the diffracted intensity is very low. To overcome these difficulties, the presented micro-beam collimator was purposely designed with a line-shaped rectangular cross-section, thin enough in one direction such that fine structure changes can be detected on scanning the sample, but sufficiently long in the other direction such that the largest number of grains is exposed for diffraction. The development is therefore particularly applicable to diffraction analyses of very thin but long sample regions, as those characteristic of unidirectional interface growth (e.g. oxide layers in tubes or metal plates), requiring the specific sample preparation.

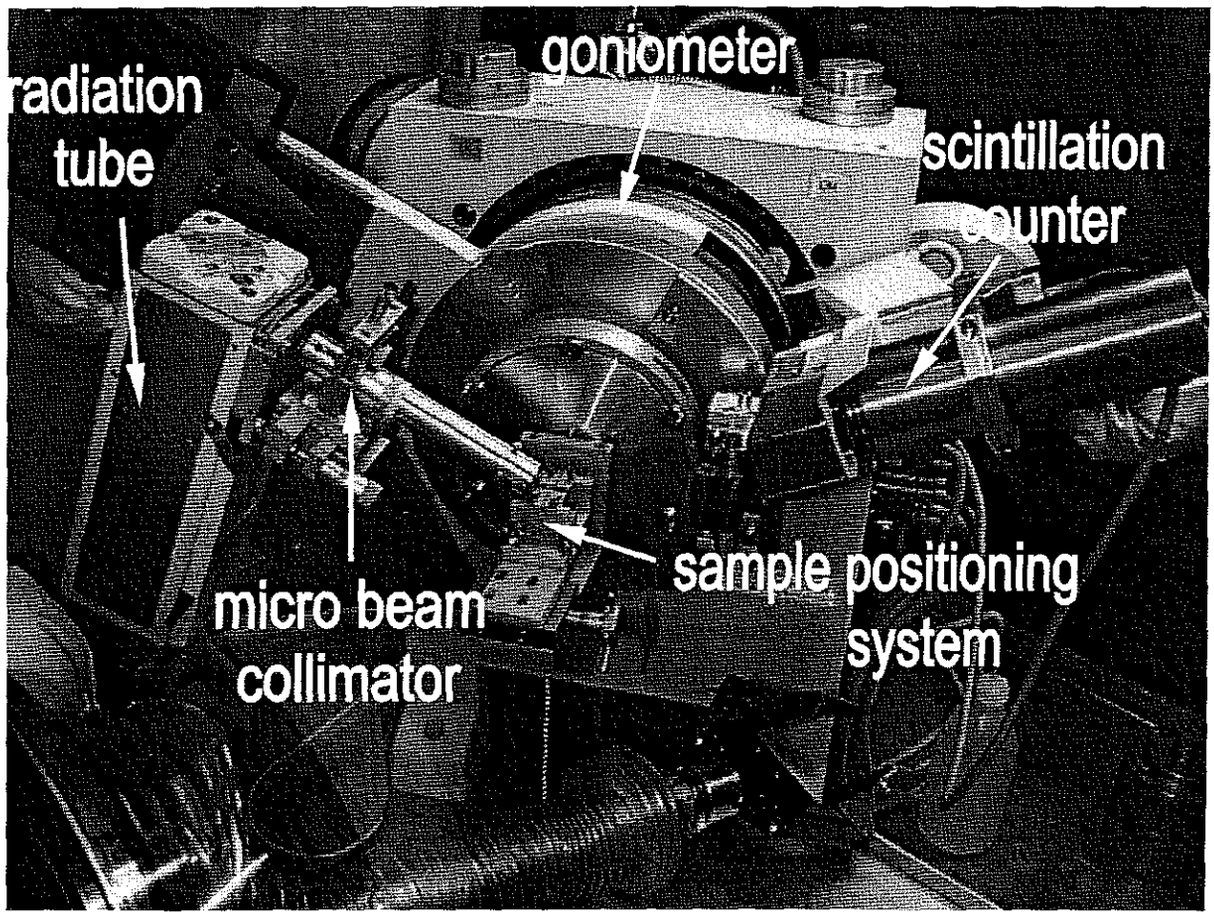

Fig. 1. The θ/θ diffractometer employed to characterise the X-ray concentrator and perform high resolution XRD investigations

[2] electron density =(Z ρ/A), where Z=atomic number, ρ=material density and A=atomic mass

The apparatus which is shown in Fig.1 has been employed to characterise and to test the formed micro-beam of the condenser. It consists of a θ/θ mode diffractometer (Seifert XRD-3000) equipped with a standard 2 KW radiation tube with line focus Cu anode and a double collimated (i.e. with anti-scatter and receiving slits) scintillation counter (Seifert SZ 20/SE). A Ni filter placed on the tube housing is utilised to eliminate the Cu-K_β wavelengths, permitting only Cu-K_α (8.05 keV) to be guided into the collimator. The X-ray micro beam collimator is mounted on the radiation tube housing by means of an angular frame and a gimbals system for fine vertical and tilt positioning. Keeping both the radiation source and detector arms at the goniometer's zero position, the condenser is oriented into the primary beam path, searching for the maximum transmitted intensity. The apparatus includes also a sample-positioning table allowing precise movements of the sample with respect to the micro beam.

3. Characteristics of the generated beam

The XRD apparatus of Fig.1 has been used to characterise the beam and to check the technique applicability under realistic operation conditions. Characterisation of the micro beam included intensity gain measurements, as well as beam divergence and spatial resolution tests.

3.1 Intensity gain

The brilliance win has been determined by comparing the intensity that is emerged from the collimator to the intensity of the primary radiation which is coming through a simple slit with the same aperture dimensions placed in the same distance from anode of the X-ray tube. For both measurements were applied the same generator parameters and the system was adjusted for maximum transmitted intensity at the goniometer zero position, with a thickness of 50 μm stainless steel foils as intensity-attenuator in the front of the detector. Under these conditions, the condenser arrangement gave an intensity of $4x10^4$ counts/s, whereas the maximum intensity of the slit configuration did not exceed $2x10^2$ counts/s. Doubtless, the 200 times higher intensity attained by the presented beam-compression system, is utilisable for hard X-rays in the range 5-30 keV. For comparison, glass monocapillary concentrators operated with conventional Cu K_α radiation sources reached only a gain of intensity of about 28 [7]. Due to this high brilliance, the condenser, often called in the text micro-beam collimator, can be operated in common X-ray diffractometers to perform high-resolution structure analysis of very thin but long solid layers or interfaces. This special kind of sample geometry appears in several technical materials applications, like in the rim region of longitudinally cut nuclear fuel pellets, oxide layers on metal plates, bonding layers in metal sheet-sandwiches, bonding layers in double-wall tubes, etc.

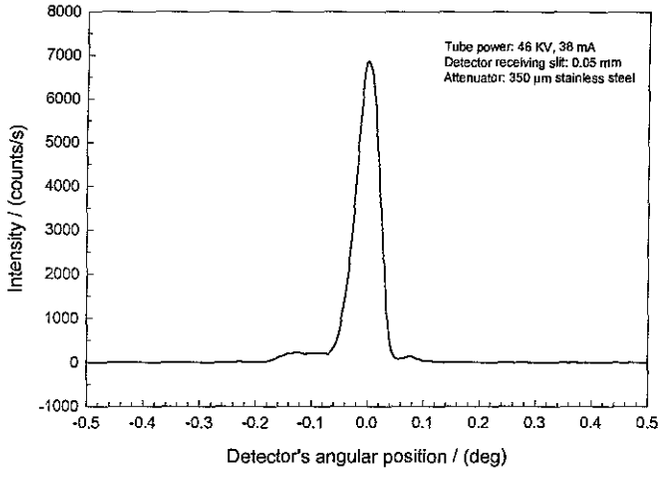

Fig. 2. Intensity profile of the generated micro beam as observed by angular detector scanning at 205 mm from the collimator exit tip

3.2 Intensity profile

The intensity profile of the generated beam measured at a distance of 205 mm from the exit of the collimator is shown in Fig.2 as a function of the departure of the detector from the angular zero position. For this intensity measurement of the direct beam, 350 µm stainless steel foils were placed as attenuator in the front of the detector in order to avoid the overflow.

It can be seen that the here presented system provides a very well defined and compact X-ray beam (needle form), without significant disturbing "satellite" peaks or increased background radiation. Due to the narrow and pure beam-profile, not only the instrument centre (zero) position can be defined therefore very precisely (a known handicap of the glass-capillary concentrated beams is the diffuse zero position [8]), but also the obtained Bragg peaks from studied samples are free of deformations and very narrow. This contributes also to obtain very precise lattice parameter measurements.

3.3 Spatial resolution and beam divergence

The spatial resolution of the micro beam collimator has been determined experimentally under the same operating conditions of routine measurements with the diffractometer of Fig.1. For this purpose, a specific sample has been prepared, consisting of a junction of two different materials, a stainless steel plate and a CaF_2 single crystal which were fixed together forming a well-defined straight interface edge.

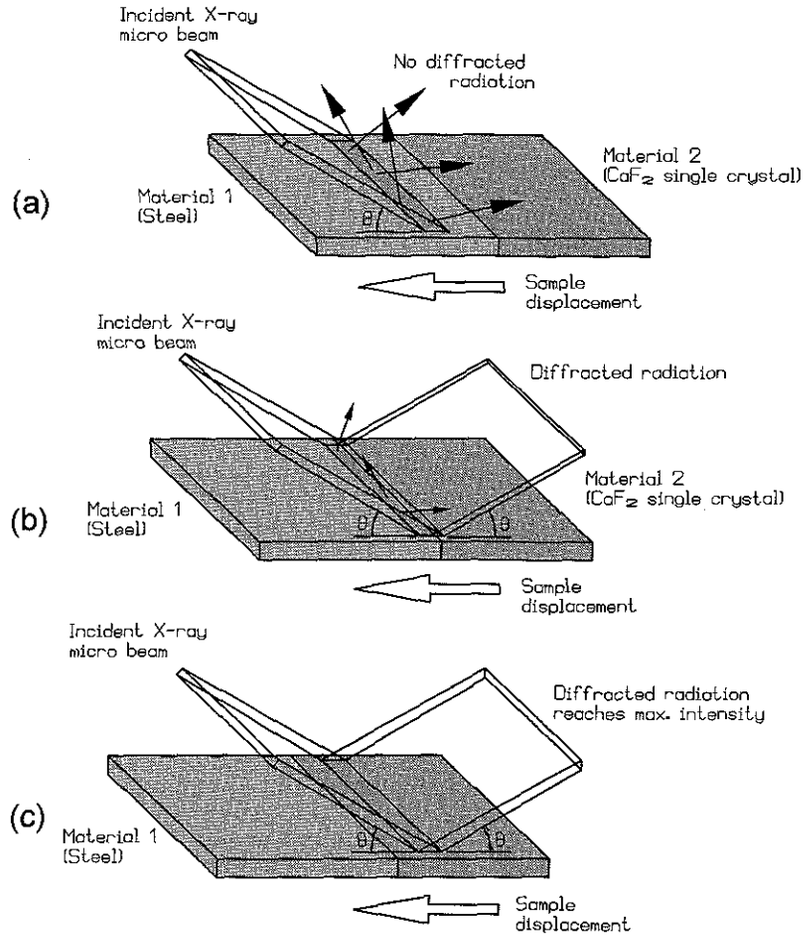

Fig. 3. Determination of the spatial resolution. (a) No diffracted signal is measured by the detector. (b) A part of the beam spot illuminates the CaF_2 crystal and the intensity of diffracted radiation is measured by the detector. (c) The diffracted signal reaches maximum intensity.

The examinations were done on the specimen after fine polishing, placing it on the translation of the sample positioning system. The goniometer arms were located at a certain pre-selected angle θ with respect to the sample surface, such that a diffracted peak for the CaF_2 single crystal was obtained. The beam spot was then positioned initially on the stainless steel plate and the sample was carefully displaced horizontally at 5 μm steps. The illuminated zone thickness (spot size) was then evaluated from the total sample displacement needed, so that the diffracted intensity varied from the background level to a maximum. (It is only to be remarked that because the prepared sample surface was not perfectly parallel to the growth-plane of the CaF_2 crystal used, the measured diffraction angles θ did correspond exactly to be tabulated Bragg-angles for CaF_2). Such intensity profiles were then obtained for several incident angles θ leading to diffracted peaks of the CaF_2 crystal, being the measured spatial resolutions plotted as a function of the incident angle as represented in Fig.4.

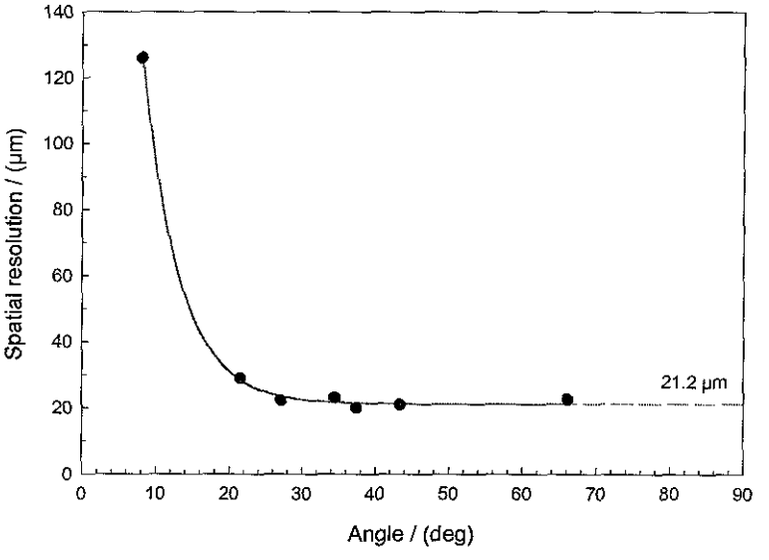

Fig. 4. Spatial resolution of the micro beam collimator as a function of beam's incident angle

The exponential decrease of the spatial resolution follows the expected dependence of the beam width projection on the sample surface with the incident angle, which is equal to the cross-section beam width divided by sinθ. Obviously, at θ=0 the projected width becomes infinite large, while at the extrapolation to θ=90° it approaches the cross-sectional beam width, which in our case is 21.2 μm (Fig.4).

Since for the spatial resolution test the sample is placed at 17 mm from the collimator exit, the obtained beam width denotes directly its low divergence. From the simple geometry of the experiment arrangement it can be easily derived that the divergence is limited to ± 0.011°. A similar result (± 0.014°) has been obtained applying the known knife edge method [7,8]. These values, certainly quite lower than the 0.32° measured for glass monocapillary concentrators under similar conditions [7,8], indicate the high compactness of the here presented micro beam.

3.4 Comparison to lead glass capillaries

Compared to glass-capillary constructions, the presented concentrator exhibits also some additional advantages. For instance, the intensity of the generated beam during operation is constant, being showed that the system is not sensible to heating effects, which in the case of glass capillaries influence negatively the throughput and disturb the transmitted signal [7]. Also, since our concentrator is made of metal, with a larger absorption coefficient, there is practically no radiation „leakage" through the reflecting walls as in the case of glass-

capillaries [2]. Radiation damages of the construction material have not been detected after several months of continuous operation, different to glass-capillaries that show darkening of the walls after a certain time [7], which could affect the efficiency and decrease the reflecting power.

Finally, the low beam divergence implies another advantage of the presented system with respect to the glass capillaries, since it allows the micro-beam device to be placed at higher distances from the sample surface without sensible loss of spatial resolution, which facilitates the whole experimental handling. As a comparison, conditioned by the larger beam divergence, similar measurements with glass capillaries are done with the exit of the capillary almost in contact with the sample [8], i.e. at a distance of 2 mm or less from the sample surface.

4. High resolution XRD investigations on nuclear spent fuels

4.1 Experimental

In the photos of Fig.5 is shown the complete installation for XRD and TG studies on radioactive samples. The diffractometer of Fig.1 and a thermobalance are installed in a glove box with 50 mm lead shielding for human protection. The XRD apparatus equipped with the micro beam collimator, a sample holding system with a micro(x,y,φ)-positioning table and a double collimated scintillation counter detector (i.e. with anti-scatter and receiving slits) has been used to carry out high resolution crystallographic investigations on the PWR spent fuel specimen of Fig.6(b) with average burn up 80 GWd/t. Since the formed micro beam is 15μmx4mm a special sample preparation is needed, presented schematically in Fig.6(a). The thickness of the embedded fuel-sample of Fig.6(b) after successive cutting and grinding-polishing operations was 0.1 mm. Inclusion of markers in the sample holder and careful control of the sample width during preparation ensured that the exposed pellet surface corresponded to the longitudinal-diametric plane

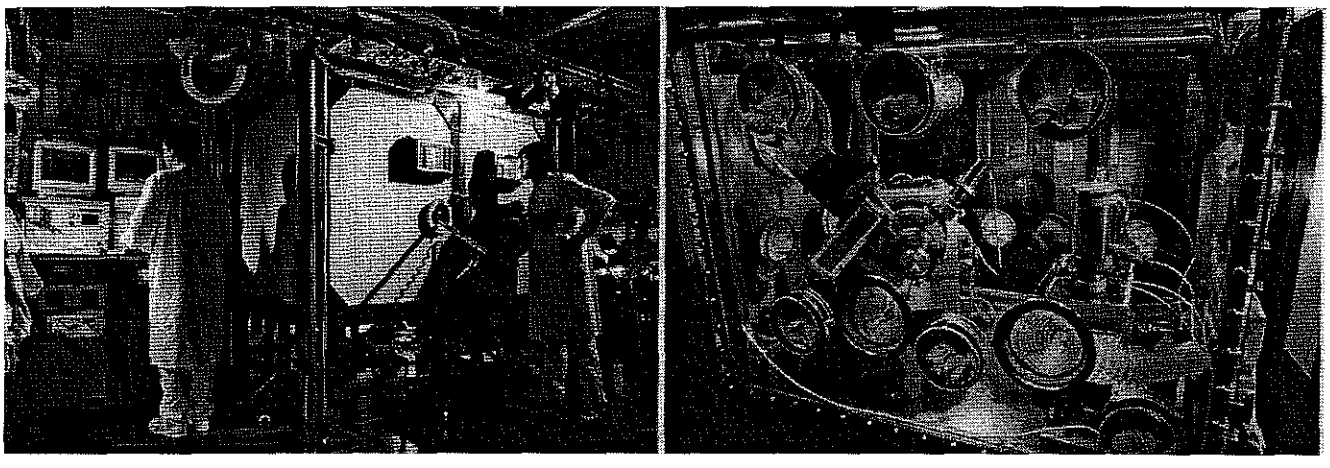

(a) (b)

Fig. 5. The lead shielded glove box. (a) Active samples are handled by manipulators. (b) A panoramic view of the installed devices.

The sample was positioned on the translation stage of the goniometer. By displacing it horizontally, a series of XRD spectra were obtained at several positions on the sample surface. The acquisition each spectrum carried out in the step-scanning mode with angular increment 0.005° and counting time 40-60 s. The spatial resolution of the system, as shown in Fig.4, guarantees that for θ>25° the projected beam width on the sample surface is 30 μm or less and sequently the obtained diffraction spectra at radial intervals 50μm can not be overlapped. A Ni-filter was utilised to eliminate the incident Cu-K_β radiation. The corresponding $K_{\alpha 1}$ and $K_{\alpha 2}$ lines for each Bragg reflection were then resolved by an appropriate peak fitting routine [10]. For lattice parameter calculations from each individual XRD spectrum, the resolved $K_{\alpha 1}$-line was used. For elimination of the systematic errors, the extrapolation function d_{hkl} vs. $\cos(\theta_{hkl})/\tan(\theta_{hkl})$ towards θ=90° was employed [11]. Apart from that, important sources of error as goniometer zero shift and eccentricity of the incident beam with respect to the goniometer axis, were eliminated by careful system alignment. The whole procedure was checked by examination of reference samples, whose lattice parameters were reproduced within an error band of ±0.01 pm.

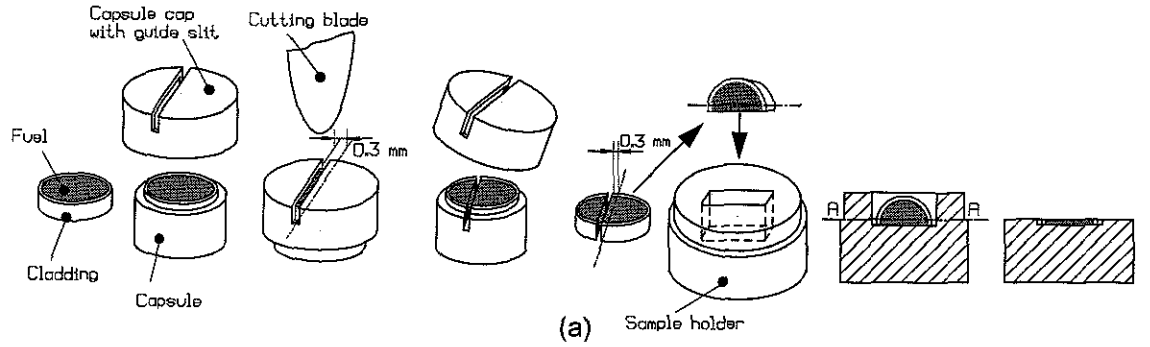

(a)

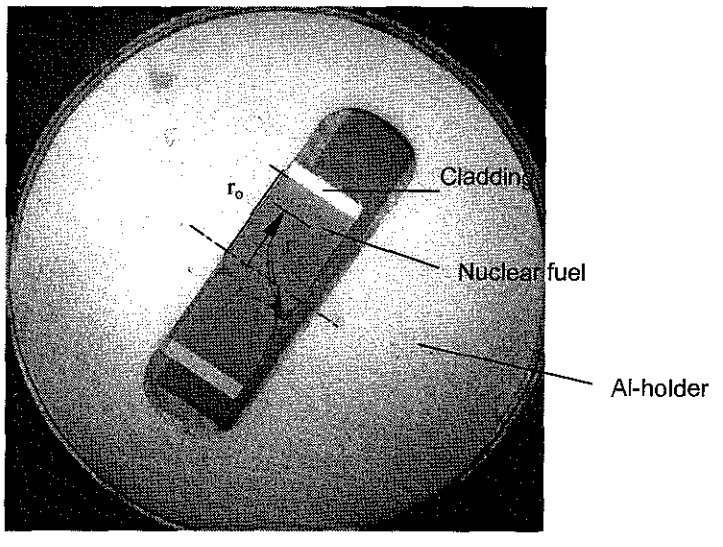

(b)

Fig. 6. (a) Schematic showing of the sample preparation for micro XRD measurements. (b) Top view of the examined spent fuel sample.

4.2 Results and short discussion

The calculated unit cell constant (parameter), as resulted from each individual XRD spectrum is given in Fig. 7 as a function of relative radial position (r/r_o) of the beam spot on the sample surface. In the same graph is also shown the average unit cell parameter (a=5.4768 Å) as observed using the conventional collimator, which illuminated the whole sample surface. Important information like irradiation data and microstructure characterisation of the examined sample can be found in the literature [12].

In Fig.7 three different radial zones can be established in terms of the lattice parameter. In the region r/r_o=0-0.52 the lattice parameter remains approximately constant, reaches a maximum at r/r_o=0.74 and decreases towards the pellet edge.

The decrease of the lattice constant toward the pellet centre is attributed to thermal healing effects. In contrast, the decrease towards the pellet edge is attributed to the formation of the rim structure, for which temperature effects are basically excluded. This is corroborated in principle by the radial profiles of the other properties (i.e. porosity, micro hardness, local burn up) showing congruent variations within the rim-zone. However, many parameters intervene in the configuration of such a profile, including the superimposed α- and fission damage, thermal healing effects, lattice dimension changes due to dissolution of fission products and actinides (Pu) and possibly oxygen in the UO_2-structure and finally the strict local burn-up effects associated with the rim-structure formation.

An attempt to give an explanation for the above radial profile of the lattice parameter is given in the literature [13]. In this section it is only briefly reported the most interest aspects and conclusions treated in detail in [13].

1) The lattice parameter of the fuel after discharge shows an important component of α-damage, which is assumed to reach its maximum at the pellet edge where the highest amount of α-emitting elements is present.
2) Above this assumed saturating α-damage, a definite lattice damage accumulation is observed in the region near the onset of the rim-zone in high burn-up fuel. This damage decreases towards both the hotter centre and the cold periphery. The decrease towards the pellet centre is attributed to thermal healing while the decrease towards the pellet edge is assigned to the formation of the rim structure.

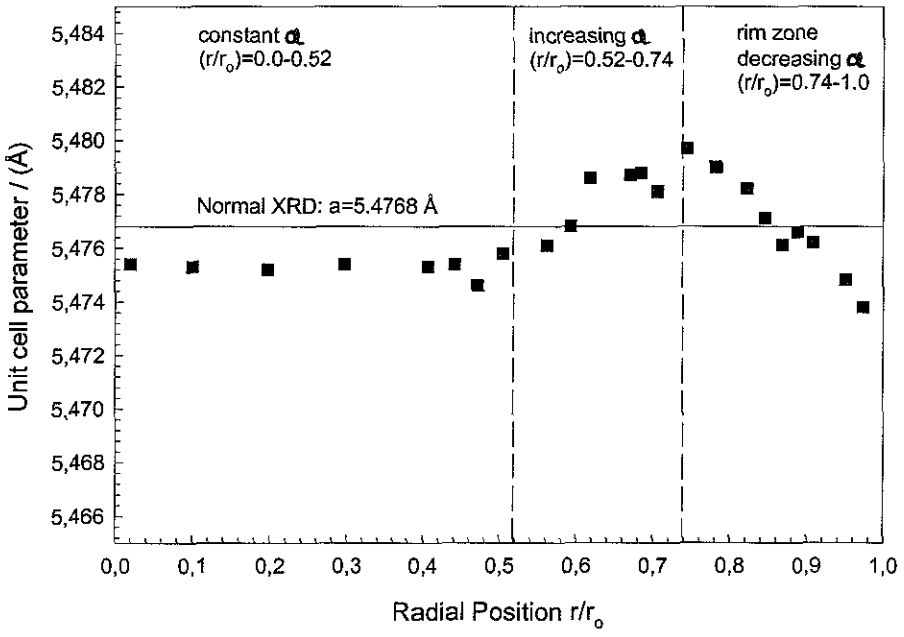

Fig. 7. Unit cell (lattice) parameter of a 80 GWd/t spent fuel as a function of radial position

3) The damage release towards the pellet edge is coincident in radial position with the evolution of other properties within the rim-zone, e.g., depletion of matrix Xe atoms, increase of porosity and decrease of hardness, etc. Moreover, in terms of local burn-ups, its rate seems basically to coincide with that of the matrix Xe depletion measured by EPMA [14]. The transfer of substantial amounts of Xe-atoms from matrix traps to pores would contribute to local strain release and sequentially to lattice parameter decrease. Since this contraction rate is much higher than that produced by dissolved foreign atoms in the lattice, solution effects are a priori excluded from the transformation.
4) The observed lattice expansion-contraction behaviour can be explained alternatively by a saturation of primary interstitial with subsequent recombination with excess vacancies, or by a number saturation and enlargement of interstitial dislocation loops. The possible explanation via dislocation loops could have a back-up in a rim structure model, assuming growth of these loops with the increase of burn-up, until saturation is reached when a stable dislocation cell structure is formed.

Literature

1. D. Bilderback, S. A. Hoffman and D. Thiel, Science, 263, (1994).
2. Naoki Yamamoto, Rev. Sci. Instrum., 67 (9), (1996).
3. P. Dhez, P. Chevallier, T.B. Lucatorto and C. Tarrio, Rev. Sci. Instrum., 70, (4), (1999).
4. D. H. Bilderback, D. J. Thiel, Rev. Sci. Instrum., 66 (2), (1995).
5. H. Klug and L. Alexander, "X-ray diffraction procedures", John Wiley & Sons, Inc., New York (1954).

6. A. H. Compton and S. K. Allison," X-rays in Theory and Experiment", D. Van Nostrand Company, Inc., (1935).
7. D. J. Thiel, D. H. Bilderback and A. Lewis, Rev. Sci. Instrum., 64 (10), (1993).
8. I. C. Noyan, P.-C. Wang, S. K. Kaldor, J. L. Jordan-Sweet and E. G. Liniger, Rev. Sci. Instrumen. , 71 (5), (2000).
9. C. A. MacDonald, S. M. Owens and W. M. Gibson, J. Appl. Cryst., 32, 160-167, (1999).
10. Seifert XDAL 3000 Software, Revision 1.4, Rich. Seifert & Co. GmbH Röntgenwerk, Ahrensbutg, Germany, (1993).
11. H. W. King, E. A. Payzant, in: J. V. Gilfrich (Ed.), Advances in X-ray Analysis, vol. 36, Plenum Press, New York, 1993, pp. 663-670.
12. R. Manzel, M. Coquerelle, in: ANS International Topical Meeting on Light Water Reactor Fuel Performance, 2-6 March, Portland, Oregon, USA (1997), pp. 463-470.
13. J. Spino, D. Papaioannou, J. Nucl. Mater., (October 2000).
14. C. Walker, J. Nucl. Mater. 98 (1981) 206.